Interleaving b and c as before gives us

"b"	11110000110011
"c"	00110011111100
$a=$"b"$+$"c"	1001011100101.

III. Comments

In the general case it was pointed out that the half-speed sequences b and c were generated by the same wiring polynomial specifying sequence a. Of course, in the special case of m-sequences, b and c will be shifts of a since, by definition, only one sequence, the maximal length sequence, is generated by a primitive wiring polynomial. If, as is often the case, the initial condition of sequence a is not important, then it is merely necessary to add bit by bit two half-speed sequences b and c, generated by the same wiring polynomial which specifies a, but with c shifted by 2^{N-1} with respect to b (in the opposite direction to the shift by $\tau/2$) as described by (13) and (14). Recall that N is the order of the wiring polynomial. The process of interleaving can, of course, be extended to interleave 4, 8, 16, etc., sequences.

These results are particularly important since many commonly used binary sequences, for example, Gold and Kasami sequences [5], can be generated by combinations of m-sequences.

References

[1] J. A. Coekin and J. R. Wicking, "Generating PRB sequences for system testing at 500 Mb/s and higher using I.C. flip flops," in *Proc. Int. Microwave Symp.*, Chicago, IL, May 1972.

[2] S. W. Golomb, *Shift Register Sequences*, rev. ed. Laguna Hills, CA: Aegean Park Press, 1982.

[3] A. Lempel and W. L. Eastman, "High speed generation of maximal length sequences," *IEEE Trans. Comput.*, vol. C-20, pp. 227-229, Feb. 1971.

[4] F. J. MacWilliams and N. J. A. Sloane, "Pseudorandom sequences and arrays," *Proc. IEEE*, vol. 64, pp. 1715-1729, Dec. 1976.

[5] D. V. Sarwate and M. B. Pursley, "Cross-correlation properties of pseudorandom and related sequences," *Proc. IEEE*, vol. 68, pp. 593-619, May 1980.

On Differential Detection of M-ary DPSK with Intersymbol Interference and Noise Correlation

JACK H. WINTERS

Abstract—**In this paper we study differential detection of M-ary differential phase-shift-keyed (DPSK) signals with intersymbol interference and noise correlation. With these impairments there can be a wide variation in the error rate of the individual symbols, with this variation increasing with M. However, by adding a phase shift offset and adjusting the decision boundaries in the detector, this variation can be reduced and the average symbol error rate can be decreased. For example, for quaternary DPSK with a signal to adjacent (from the previous and next symbols) intersymbol interference power ratio of 17 dB, these methods can reduce the variation in symbol error rates by more than two orders of magnitude and decrease the required signal-to-thermal noise ratio for a 10^{-6} symbol error rate by more than 2 dB.**

Paper approved by the Editor for Data Communications and Modulation of the IEEE Communications Society. Manuscript received July 30, 1985; revised August 8, 1986. This paper was presented at the IEEE International Conference on Communications, Amsterdam, The Netherlands, May 1984.

The author is with AT&T Bell Laboratories, Holmdel, NJ 07733.

IEEE Log Number 8611693.

I. Introduction

Differential detection of differential phase-shift-keyed (DPSK) signals with noise correlation and/or intersymbol interference (or power imbalance[1]) has been extensively studied (e.g., [1]-[11]). However, most of these papers consider only the *average* symbol error rate for *conventional* DPSK (with $2n\pi/M$, $n = 0, \cdots, M-1$ phase shifts with respect to the previous symbol).

For all M-ary DPSK techniques (except symmetrical binary DPSK with $\pm\pi/2$ phase shifts), because of the lack of symmetry of the phase shifts for the symbols, the symbol error rate is not the same for all symbols with intersymbol interference [12]-[14] or noise correlation [7]. The variation in the symbol error rates is undesirable and complicates the design of error-correcting codes. The decision regions in the detector can be adjusted, however, to reduce this variation and, at the same time, reduce the average symbol error rate [11].

The effect of intersymbol interference and noise correlation on the individual and average symbol error rates depends on M, the decision regions in the detector, the phase shift offset angle (a fixed phase shift added to each symbol interval), and the type of intersymbol interference and noise correlation. Although considering all possible cases for these parameters is impossible, studies of the effect of these parameters on the symbol error rates showed several interesting features as described below, which will be illustrated by studying binary and quaternary DPSK with adjacent intersymbol interference (as in [8] and [10]) and noise correlation.

II. Differential Detection

At the transmitter, an M-ary DPSK signal can be written as

$$s(t)=A\ \sin\ (\omega_0 t+\alpha(t)) \tag{1}$$

where A is an amplitude constant, ω_0 is the carrier radian frequency, and $\alpha(t)$ is the message-carrying waveform. For the mth symbol interval of T_s seconds (i.e., $(m-1)T_s < t \leq mT_s$), the message carrying waveform is given by

$$\alpha(t)=\alpha_m=\alpha_{m-1}+\phi_0+\frac{2\pi}{M}\,d_m \tag{2}$$

where ϕ_0 is the phase shift offset angle and d_m is the mth data symbol, where $d_m = 0, \cdots, M-1$.

Fig. 1 shows the differential detector analyzed in this paper.[2] The received signal $z(t)$, consisting of a distorted DPSK signal and noise, is split into quadrature baseband components. The components are then integrated to generate the symbol signal vector components. The mth symbol signal vector is therefore given by

$$\bar{z}_m=e_{x_m}\bar{a}_x+e_{y_m}\bar{a}_y \tag{3}$$

where $\bar{a}_x$ and $\bar{a}_y$ are unit vectors defining a rectangular coordinate frame, and e_{x_m} and e_{y_m} are the coefficients of these

[1] With intersymbol interference, the power imbalance (between two adjacent symbol signal vectors used to determine the phase shift) is dependent on the symbol sequence.

[2] The differential detector studied in many papers is often of another form, that shown in Fig. 2. Our results also apply to this detector, where signal samples and complex phasor notation are employed (see, e.g., [9], [11]). Note that for the detector of Fig. 1, the decision regions can be easily adjusted, unlike the detector of Fig. 2.

0090-6778/87/0100-0117$01.00

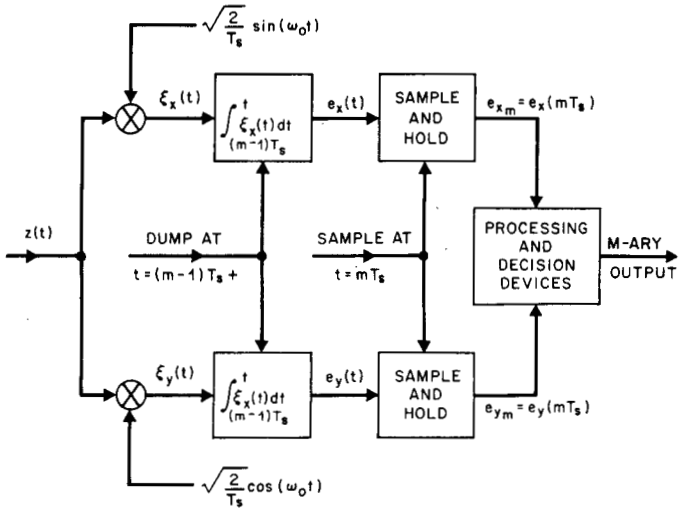

Fig. 1. The differential detector analyzed in this paper.

vectors, as shown in Fig. 1. Thus, the phase of $\bar{z}_m$ is the arctangent of the ratio of the symbol signal vector components. The detection statistic ψ is the phase difference[3]

$$\psi = \angle \bar{z}_m - \angle \bar{z}_{m-1} \tag{4}$$

where $\angle$ denotes the angle of the vector. The decision rule is then given by

$$\psi_{0(d-1)d} < \psi - \phi_0 \le \psi_{0d(d+1)}, \quad \text{"}d\text{" transmitted, } d=0, \cdots, M-1 \tag{5}$$

where $\psi_{0_{ab}}$ is the decision boundary angle between symbols a and b, and $d-1$ and $d+1$ are modulo M. Let

$$\bar{z}_m = \bar{S}_m + \bar{N}_m \tag{6}$$

where $\bar{S}_m$ and $\bar{N}_m$ are the signal and noise vectors for the mth symbol. We consider adjacent intersymbol interference, with the normalized intersymbol interference from the previous symbol ΔL_p and the next symbol ΔL_n given by

$$\Delta L_{p,n} = \frac{\int_{t_0-T_s}^{t_0} x(t \pm T_s)\, dt}{\int_{t_0-T_s}^{t_0} x(t)\, dt} \tag{7}$$

with the minus and plus signs for ΔL_p and ΔL_n, respectively, where $x(t)$ is the overall pulse (of duration T_s) response of a given system and t_0 is the sampling time. Thus, with adjacent intersymbol interference, the two signal vectors that determine the mth symbol, $\bar{S}_{m-1}$ and $\bar{S}_m$, depend on three symbols, d_{m-1}, d_m, and d_{m+1}, and can easily be shown to be given by

$$\bar{S}_i = \sqrt{E_s}\,[\cos(\alpha_i) + j\sin(\alpha_i) + \Delta L_p(\cos(\alpha_{i-1}) + j\sin(\alpha_{i-1})) + \Delta L_n(\cos(\alpha_{i+1}) + j\sin(\alpha_{i+1}))] \tag{8}$$

for $i = m-1$ and m, respectively, where E_s is the energy per symbol without intersymbol interference. Furthermore, we consider only noise correlation between adjacent symbol intervals, i.e., the noise correlation r is given by

$$r = E[\bar{N}_m \cdot \bar{N}_{m-1}]/N_0 \tag{9}$$

where $E[\cdot]$ denotes expected value, and N_0 is the single-sided noise power spectral density. From [1, eq. (7)–(9)] the symbol

[3] All angles are modulo 2π.

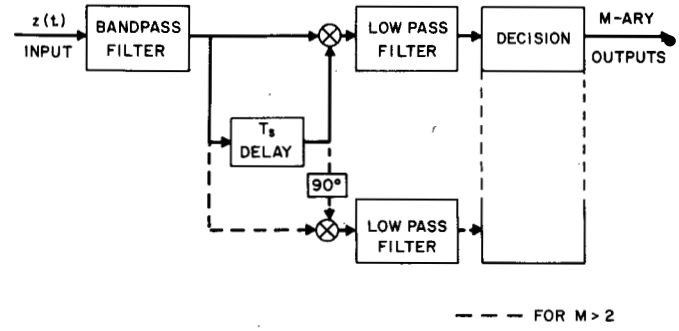

Fig. 2. A second possible implementation of the differential detector.

error rate for the mth data symbol for a given symbol sequence is given by

$$P(E|\text{symbol sequence}) = F[\psi_{0d_m(d_{m+1})} + \phi_0 | \Delta\Phi] - F[\psi_{0(d_{m-1})d_m} + \phi_0 | \Delta\Phi] \tag{10}$$

where $F(\phi|\Delta\Phi)$ is given by [1, eq. (8), (9)]. (Simplified formulas for specific cases are given in [11, eq. (14)] and [9, eq. (5)–(7)].) Note that since [1] studies the detector of Fig. 2, to use the analysis of [1], $|\bar{S}_m|^2/2N_0$ must be replaced by $p(t)$ and $\angle \bar{S}_m$ by $\phi(t)$. With adjacent intersymbol interference, the probability of error for a given symbol d is the average probability of error for the 2^M symbol sequences (of length 3) with d as the second symbol.

III. Effect of Intersymbol Interference and Noise Correlation on M-ary DPSK

We now study the variation in the individual symbol error rates and the average error rate with intersymbol interference and noise correlation, and consider the effect of the phase shift offset angle ϕ_0, the number of phases M, and the decision boundary angles $\psi_{0_{ab}}$. These effects are illustrated in Figs. 3–8 for $\Delta L_p = \Delta L_n = 0.1$ (17 dB signal-to-interference power ratio) and $r = 0.1$ and where $E_b = E_s/\log_2 M$ is the energy per bit.

Consider first the variation in the individual symbol error rates. With conventional ($\phi_0 = 0$) DPSK and positive noise correlation with intersymbol interference, the difference in error rates for "0's" and "1's" is greater than with either impairment alone. As M increases, the variation in the individual symbol error rates increases (for the same intersymbol interference and noise correlation). For fixed M, as ϕ_0 increases, the variation decreases, with a minimum variation for $\phi_0 = \pi/M$. (With symmetrical ($\phi_0 = \pi/2$) binary DPSK, the error rates for "0's" and "1's" are equal.) For example, from Figs. 3–5 at $E_b/N_0 = 14$ dB, the symbol error rates vary by a factor of 900 and 1400 for conventional ($\phi_0 = 0$) binary and quaternary DPSK, respectively, and by a factor of 40 for quaternary DPSK with $\phi_0 = \pi/4$.

As discussed previously, since the symbol error rates vary (except for symmetrical binary DPSK), the decision boundary angles can be adjusted to reduce this variation and also reduce the average error rate. Here, we consider adjusting the angles to minimize the average symbol error rate (for given M, ϕ_0, ΔL_p, ΔL_n, and r). With the optimum decision boundary angles, the variation in the individual symbol error rates is also significantly reduced, although the individual symbol error rates are not necessarily equal. For example, from Figs. 6 and 7, with the optimum decision boundary angles the individual symbol error rates vary by a factor of only 5 and 10 with conventional binary and quaternary DPSK, respectively. With the optimum angles the variation is again less with $\phi_0 = \pi/M$, a factor of only 4 for quaternary DPSK.

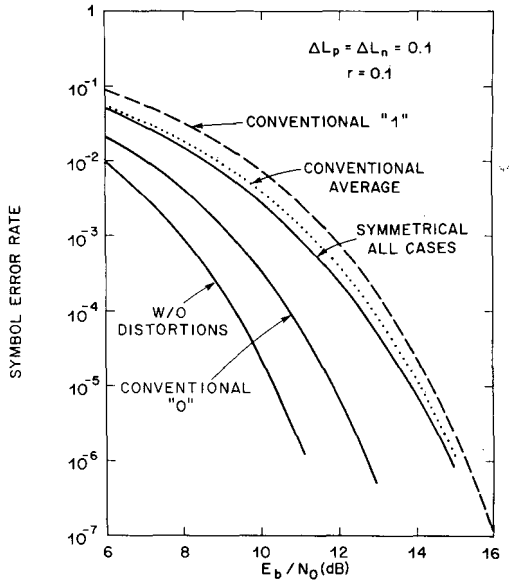

Fig. 3. The symbol error rate versus the energy-per-bit-to-noise-density ratio for conventional and symmetrical binary DPSK with ΔL_p, ΔL_n, and r equal to 0.1. The error rate of a "1" is much greater than that for a "0" with conventional DPSK, but the error rates are equal for symmetrical DPSK.

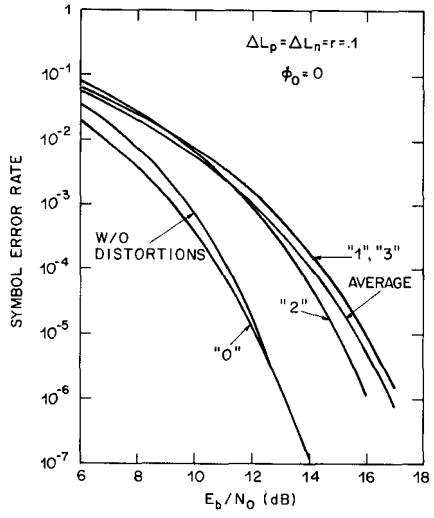

Fig. 4. The symbol error rate versus the energy-per-bit-to-noise-density ratio for conventional quaternary DPSK and ΔL_p, ΔL_n, and r equal to 0.1.

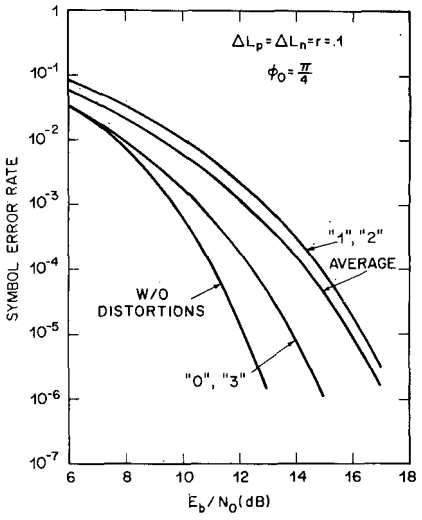

Fig. 5. The symbol error rate versus the energy-per-bit-to-noise-density ratio for quaternary DPSK with $\phi_0 = \pi/4$ and ΔL_p, ΔL_n, and r equal to 0.1.

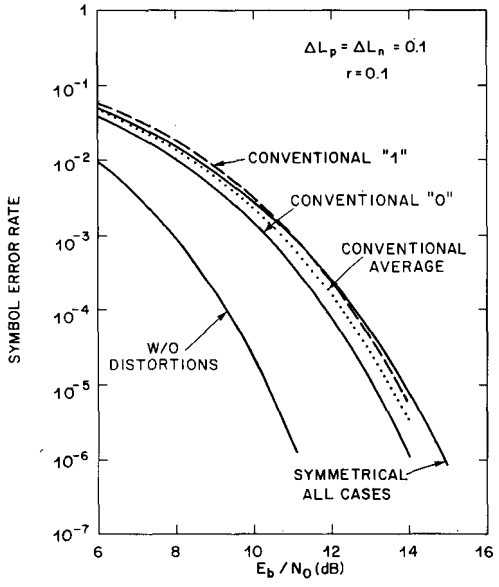

Fig. 6. The symbol error rate versus the energy-per-bit-to-noise-density ratio for conventional binary DPSK with optimum ψ_0 and for symmetrical binary DPSK with ΔL_p, ΔL_n, and r equal to 0.1. The difference in error rates for "0's" and "1's" is much less than that shown in Fig. 3, and the average symbol error rate for conventional DPSK is also lower.

Next consider the average symbol error rate. For binary DPSK the average error rate varies slightly with ϕ_0, with the ϕ_0 for minimum error rate depending on the intersymbol interference and noise correlation. For small ΔL_p, ΔL_n, and r, symmetrical binary DPSK has the lowest error rate, while for large ΔL_p, ΔL_n, and r, conventional binary DPSK is lower. However, for $M \geq 4$, the effect of ϕ_0 on the average symbol error rate is negligible (as shown in [1]). On the other hand, optimization of the decision boundary angles can significantly reduce the average symbol error rate, especially for $M > 2$. For example, from Figs. 3–8, with conventional binary DPSK, optimization of the decision boundary angles reduces the required E_b/N_0 for a 10^{-6} error rate by 0.6 dB (from 15.1 to 14.5 dB), such that conventional binary DPSK has a lower error rate than symmetrical binary DPSK. For quaternary DPSK, optimization of the decision boundary angles reduces the required E_b/N_0 for a 10^{-6} error rate by 2 dB (from 16.9 to 14.9 dB). Note that although the optimum decision boundary angles vary widely with ϕ_0, with these angles the average symbol error rate does not vary significantly with ϕ_0.

IV. Summary and Conclusions

In this paper we have studied the variation in the individual symbol error rates and the average error rate for M-ary DPSK with intersymbol interference and noise correlation. Although the individual symbol error rates can vary by orders of magnitude, this variation can be significantly reduced by using a phase shift offset angle of π/M and also by adjusting the decision boundary angles in the detector. Although the phase offset angle has little effect on the average symbol error rate, adjustment of the decision boundary angles can significantly reduce the degradation in error rate performance due to intersymbol interference and noise correlation, particularly for $M > 2$.

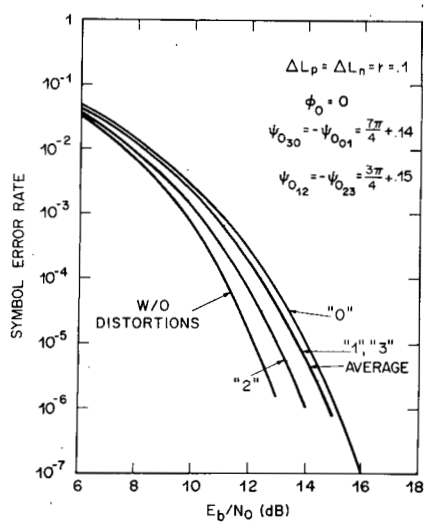

Fig. 7. The symbol error rate versus the energy-per-bit-to-noise-density ratio for conventional quaternary DPSK with optimum decision boundary angles with ΔL_p, ΔL_n, and r equal to 0.1. The difference in the individual symbol error rates is much less than that shown in Fig. 4, and the average symbol error rate is also lower.

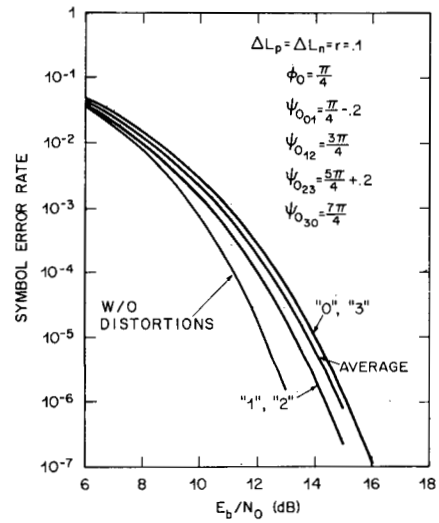

Fig. 8. The symbol error rate versus the energy-per-bit-to-noise-density ratio for quaternary DPSK with $\phi_0 = \pi/4$ for optimum decision boundary angles with ΔL_p, ΔL_n, and r equal to 0.1. The difference in the individual symbol error rates is much less than that shown in Fig. 5, and the average symbol error rate is also lower.

References

[1] R. F. Pawula, "On M-ary DPSK transmission over terrestrial and satellite channels," *IEEE Trans. Commun.*, vol. COM-32, pp. 752–761, July 1984.

[2] W. M. Hubbard, "The effect of intersymbol interference on error rate in binary differentially-coherent phase-shift-keyed systems," *Bell Syst. Tech. J.*, vol. 46, pp. 1149–1172, July–Aug. 1967.

[3] O. Shimbo, M. I. Celebiler, and R. J. Fang, "Performance analysis of DPSK systems in both thermal noise and intersymbol interference," *IEEE Trans. Commun. Technol.*, vol. COM-19, pp. 1179–1188, Dec. 1971.

[4] G. J. Marshall, "Problems of receiver-filter design for a digitally modulated carrier system," *J. Sci. Technol.*, vol. 38, no. 4, pp. 174–182, 1971.

[5] J. S. Lee and L. E. Miller, "On the binary communication systems in correlated Gaussian noise," *IEEE Trans. Commun.*, vol. COM-23, pp. 255–259, Feb. 1975.

[6] V. K. Prabhu and J. Salz, "On the performance of phase shift-keying systems," *Bell Syst. Tech. J.*, vol. 60, pp. 2307–2343, Dec. 1981.

[7] J. S. Lee, R. H. French, and Y. K. Hong, "Error performance of differentially coherent detection of binary DPSK data transmission on the hard-limiting satellite channel," *IEEE Trans. Inform. Theory*, vol. IT-27, pp. 489–497, July 1981.

[8] B. T. Tan and T. T. Tjhung, "On binary DPSK error rates due to noise and intersymbol interference," *IEEE Trans. Commun.*, vol. COM-31, pp. 463–466, Mar. 1983.

[9] R. F. Pawula and J. H. Roberts, "The effects of noise correlation and power imbalance on terrestrial and satellite DPSK channels," *IEEE Trans. Commun.*, vol. COM-31, pp. 750–755, June 1983.

[10] K. M. Lye and T. T. Tjhung, "On quaternary DPSK error rates due to noise and interference," in *Proc. Int. Conf. Commun.*, Toronto, Ont., Canada, June 1986, pp. 50.1.1–50.1.4.

[11] R. F. Pawula, "Offset DPSK and a comparison of conventional and symmetric DPSK with noise correlation and power imbalance," *IEEE Trans. Commun.*, vol. COM-32, pp. 233–240, Mar. 1984.

[12] R. J. Huff, "An investigation of time division multiple access space communications systems," Ph.D. dissertation, Ohio State Univ., Columbus, 1969.

[13] J. H. Winters, "On the performance of an imperfectly-implemented symmetrical differential detector," ElectroSci. Lab., Dep. Elec. Eng., Ohio State Univ., Columbus, Rep. 710300-3, Aug. 1978; prepared under Contr. F30602-75-C-0061 for Rome Air Develop. Cen., Griffiss AFB, NY.

[14] ——, "Differential detection with intersymbol interference and frequency uncertainty," *IEEE Trans. Commun.*, vol. COM-32, pp. 25–33, Jan. 1984.

A Nonslotted Random-Access Channel with Higher Utilization

ALEKSANDER T. KOZLOWSKI

Abstract—**The paper considers a nonslotted random-access radio channel with users divided into a few classes. Assuming that capture exists between these classes of users and that users allotted to different classes use packets of different lengths, packet and data throughput are obtained. A set of packet lengths is found for which these throughputs exceed throughputs in the case when all users use equal-length packets. Finally, the sets of packet lengths and class traffics are obtained to give the global maximum channel utilization.**

Introduction

Let us consider a random-access radio channel (RAC) like the one used in nonslotted ALOHA [1]–[3]. All channel users are divided into K disjoint classes denoted 1, 2, $\cdots$, K at different power levels in such a way that if $k < n$, k, $n = 1$, 2, $\cdots$, K, kth-class packets always dominate nth-class packets. Such a model of the system was first analyzed by Metzner [3] under the assumption that all system packets are of equal length. In contrast to that analysis we will assume that, although all the users allotted to one class use packets of equal length, different classes may nevertheless use packets of different lengths.

Paper approved by the Editor for Computer Communication of the IEEE Communications Society. Manuscript received May 23, 1985; revised July 15, 1986.

The author is with the Institute of Telecommunications, Technical University of Gdansk, Gdansk, Poland.

IEEE Log Number 8611694.